Laboratory Study of the Impact of the Cathode Grade on the Formation of Deposits on the Cathode Surface in Hall-Héroult Cells

Jean-René Landry, Mojtaba Fallah Fini, Gervais Soucy, Martin Désilets, Patrick Pelletier, Loig Rivoaland, and Didier Lombard

Abstract

This experimental study investigates the effect of the cathode grade on the formation of deposits at the carbon aluminium interface in Hall-Héroult electrolysis cells. Five different industrial cathode grades are tested in a bench scale aluminum electrolysis setup with the following operational parameters: cathodic current density of 0.9 A/cm^2, under a nitrogen atmosphere at 960 °C for 8 h with initial bath composition of 9% alumina, cryolite ratio of 2.18 and 5% CaF$_2$. Post mortem analyses include X-Ray diffraction on the ledge toe, side ledge, sludge and bath samples as well as scanning electron microscopy-energy dispersive spectroscopy and optical microscopy of the carbon aluminum interface. Early results suggest that the thickness of the aluminium carbide layer increases with the porosity of the carbon material. Secondly, the amount of sludge seems to be more related to the cathode grade than to the other operational parameters such as the temperature.

Introduction

The formation of deposits on the surface of the cathode in Hall-Héroult cells is a phenomenon that disturbs the electrical current paths and accelerates the cathode wear [1, 2]. Nowadays, for high amperage cells, the industry is leaning towards graphitized types of cathode blocks because of their higher thermal conductivity and low electrical resistivity compared to semi-graphitic or graphitic types of cathode [3]. Although the physical properties have improved, the formation of deposits on the cathode surface is still an ongoing problem at the industrial level. Investigations on this problem often focus on the operating conditions of the cell and little on the equipment type such as cathode grade. The industry has reported different behaviours among graphitized cathode types regarding deposit formation. This may be attributed to the differences in properties such as porosity, permeability or thermal conductivity. These differences may induce various behaviours in the electrolyte, thus potentially affecting the formation of deposits [4].

Distinct types of deposits at the carbon-aluminium interface have been identified:

(a) The formation of a layer of aluminium carbide (Al$_4$C$_3$) infiltrated in the carbon block has been established [5]. Moreover, it is stipulated that the combined formation and dissolution of this layer wears off the carbon surface of the block. Also, the use of graphitized blocks result in a higher wear of the cathodic carbon block [6]. Aluminium carbides are formed by the contact of the metal with the carbon interface (Eq. 1) or by the interaction of carbon with the intercalated bath components according to reactions 2 and 3 [7].

J.-R. Landry · M. Fallah Fini · G. Soucy (✉) · M. Désilets
Université de Sherbrooke, Sherbrooke, Canada
e-mail: Gervais.Soucy@USherbrooke.ca

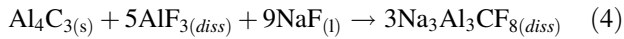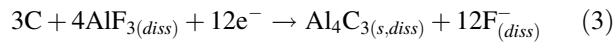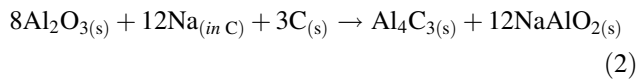J.-R. Landry
e-mail: Jean-Rene.Landry@USherbrooke.ca
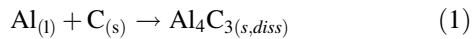
M. Fallah Fini
e-mail: Mojtaba.Fallah.Fini@USherbrooke.ca

M. Désilets
e-mail: Martin.Desilets@USherbrooke.ca

L. Rivoaland
Carbone Savoie, Venissieux, France
e-mail: loig.rivoaland@carbone-savoie.com

P. Pelletier
Rio Tinto, Jonquière, QC, Canada
e-mail: Patrick.Pelletier3@riotinto.com

D. Lombard
Rio Tinto, Saint Jean de Maurienne, France
e-mail: didier.lombard@riotinto.com

$$Al_{(l)} + C_{(s)} \rightarrow Al_4C_{3(s,diss)} \tag{1}$$

$$8Al_2O_{3(s)} + 12Na_{(in\ C)} + 3C_{(s)} \rightarrow Al_4C_{3(s)} + 12NaAlO_{2(s)} \tag{2}$$

$$3C + 4AlF_{3(diss)} + 12e^- \rightarrow Al_4C_{3(s,diss)} + 12F^-_{(diss)} \tag{3}$$

$$Al_4C_{3(s)} + 5AlF_{3(diss)} + 9NaF_{(l)} \rightarrow 3Na_3Al_3CF_{8(diss)} \tag{4}$$

The subsequent dissolution of aluminium carbides is described by Eq. 4.

(b) In addition, the presence of sludge in the center of aluminium reduction cells is often found under alumina point feeders. It is often said to be caused by the cover material falling during anode changes. It is also thought to be attributed to incomplete dissolution of alumina, leading to agglomerates, which may carry bath components through the metal pad down to the carbon interface [2, 8]. Aluminium carbides may dissolve in the sludge found under the aluminium [9].

(c) Furthermore, the heat losses through sidewalls and bottom of cell may cause the side ledge to grow at the carbon-aluminium interface [10]. The impact of all these phenomena is the enhanced erosion of the block at the tip of the frozen ledge and disturbed current paths with an increase in cathode voltage drop [11, 12].

The formation of these deposits are certainly affected by the cathode block properties. This experimental study will investigate the role of the cathode grade by making further links between specific properties of the block and the formation of deposits.

Methodology

Experimental Setup

Aluminium electrolysis tests are done using five industrial cathode grades (A, B, C, D and E). Grades A–D are graphitized block grades with several coke sources and E is impregnated graphite (block graphitized then impregnated with pitch and rebaked). The properties of these grades were given by the supplier and are listed in Table 1.

The propensity to form sludge by grade by each grade generally seen in industry is D = E > A > B > C, D and; D and E being the grades that equally form the most sludge. This study aims to evaluate the behavior of the experimental cells for comparison with the real life behavior reported.

Rectangular experimental blocks of the five grades have been machined for laboratory electrolysis tests. All dimensions of the cell components are shown in Fig. 1.

The cell is filled with 1700 g of industrial bath initially containing 9% (w/w) alumina with a cryolite ratio (CR) of 2.18. A block of approximately 500 g of aluminium is placed at the bottom of the cell prior to the electrolysis and 5 mm thick alumina plates cover all vertical walls of the carbon block to limit bath infiltrations. The cell is positioned inside a crucible made of Inconel placed inside an oven. The

Table 1 Cathode block properties at room temperature

Properties	A	B	C	D	E
Thermal conductivity (W/m K)	125[a] 112[b]	130[a] 115[b]	145[a] 135[b]	130[a] 105[b]	130[a] 105[b]
Open porosity (%)	18	14	15	20	14
Air permeability (nPerm)	8	7	3	6	5

[a]Horizontal, [b]vertical

Fig. 1 Sizing of experimental Hall-Héroult cell for this study, top view (a) and side view (b). All dimensions are in millimeters (mm). 1 carbon crucible, 2 alumina plates, 3 anode, 4 bath, 5 aluminium
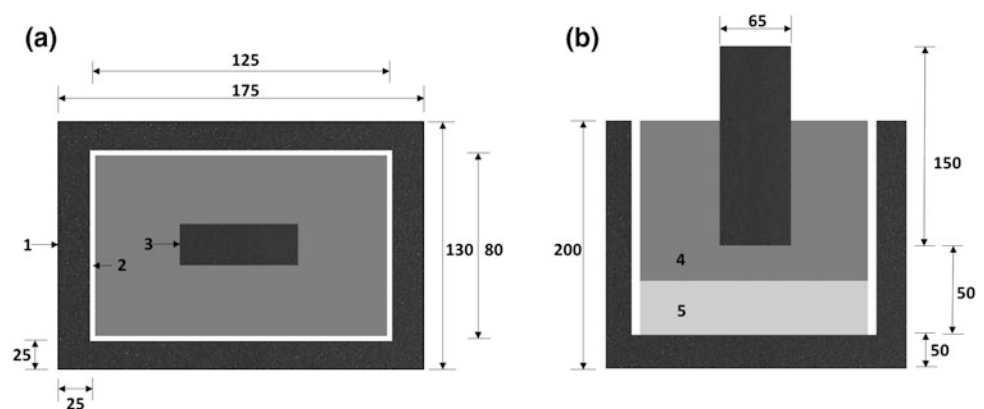
temperature is measured in three locations: inside the bath, in the carbon sidewall and outside the cell.

The electrolysis tests are done at a bath temperature of 960 °C, a current density of 0.9 A/cm^2 for 8 h under a N$_2$ atmosphere. The current is set to 73 A and is kept constant. The temperature and voltage are measured continuously during electrolysis. In all cases, a sudden increase in temperature up to 970 °C is observed at the beginning of electrolysis, which may be attributed to Joule effect. The temperature reaches then 960 °C and is kept stable during electrolysis. The anode to cathode distance is set to 2 cm. In order to highlight the impact of the cathode grade, no feeding is used and all parameters are kept constant during the cell operation for all cathode grades.

Autopsies and Characterization

At the end of the electrolysis time, the electricity is cut off and the furnace is set to room temperature for cooling. In order to observe the deposits at the carbon-aluminium interface, the cooled cell is cut using a diamond blade saw. Cuts are made in the center of the cell and in periphery. Each section of the carbon-aluminium interface is observed with a stereomicroscope. Pictures are taken to recreate panoramic views of the interface. For composition, harvested samples are powdered using a ball mill then put in the rotating sample holder of the X-Ray diffraction (XRD). The chemical composition is provided by the Rietveld analysis of the sample. Scanning electron microscopy-energy dispersive spectroscopy (SEM-EDS) was used for surface analysis and elemental cartography. This method of analysis allows observation and easy measurements of the aluminium carbide layer in the carbon block.

Results

Aluminium Carbide Observation

Scanning electron microscopy was used to observe the carbon-aluminium interface. For each site of interest, the elemental cartography included mapping of carbon, aluminium, oxygen, fluoride, calcium and sodium. Figure 2 shows the observable carbide layer.

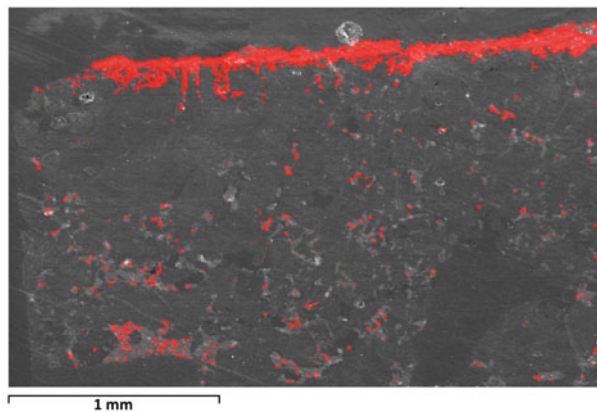A noticeable distinct red layer containing atoms of aluminium was visible at the interface for every sample

Fig. 2 Scanning electron microscopy of the carbon-aluminium interface of experimental cell E (impregnated graphite). The position of the aluminium carbide layer is shown by the bracket symbol

taken. The values of the measured thickness of the carbide layer for each cathode grade are summarized in Table 2. The following data were obtained by averaging all direct measurements of the layer. The samples were taken under the sludge, under the ledge toe and in the "cleaner" areas in between (direct contact of aluminium and carbon).

The impregnated graphite grade had the sharpest and most distinct layer of aluminium carbide. Other graphitized grades had a dispersed carbide layer.

Ledge and Sludge Observations

Microscopic observations revealed the presence of sludge accumulated near the center of the carbon-aluminium interface under the anode tip. Typical profiles of sludge are exhibited in Fig. 3.

All grades displayed a central deposit of sludge. As indicated in Table 3, graphitized grade A had the thickest central sludge with a thick bath film covering the carbon-aluminium interface and thicker ledge. The experimental cell of grade A had the highest sludge propensity and the four other grades showed thinner layer than grade A. At this stage, it is difficult to conclude a sludge propensity trend between the other grades.

For each experiment, the central deposit was harvested along with a ledge toe sample from the same cell. The CR and alumina content of these samples are also summarized in Table 3.

Table 2 Average aluminium carbide layer thickness (±4 μm). The average data for two tests of each grade is displayed

Cathode type	Graphitized				Impregnated graphite
Cathode grade	A	B	C	D	E
Carbide layer thickness (μm)	54 | 55	65 | 66	41 | 48	89 | 96	65 | 72

Fig. 3 Typical sludge profiles for graphitized grade A (**a**), impregnated graphite grade E (**b**)
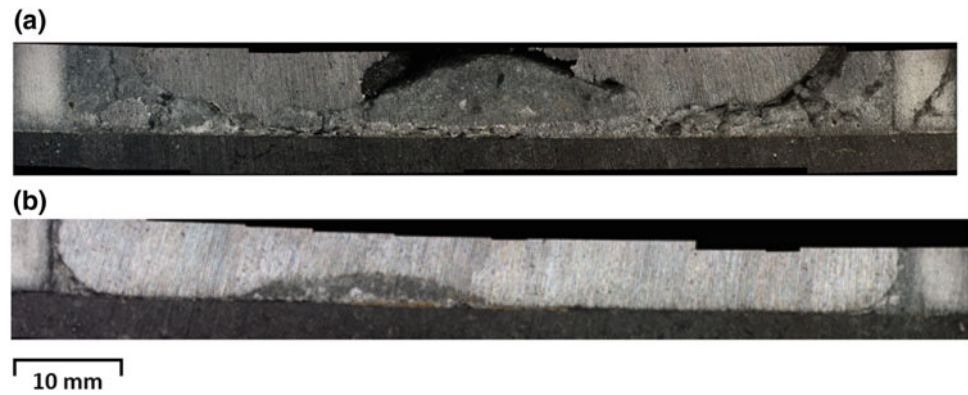

Table 3 CR, total alumina content and height of ledge toe and central sludge deposits from XRD-Rietveld analysis

	Ledge toe		Central sludge		
	CR	Total Al_2O_3 (%)	CR	Total Al_2O_3 (%)	Height ($\pm$ 0.5 mm)
A (graphitized)	2.87	25.0	2.09	10.2	8.1
B (graphitized)	2.87	23.3	2.92	9.8	3.4
C (graphitized)	2.73	27.4	2.95	11.4	4.7
D (graphitized)	2.85	21.4	2.79	13.5	3.2
E (imp. graphite)	2.12	28.8	2.08	19.1	5.1

Discussion

Aluminium Carbide Layer—Effect of Porosity

The data for the thickness of the aluminium carbide layer has been plotted in Fig. 4.

Measurements for graphitized cathode blocks A, C and D show a trend between the block's open porosity and the thickness of the aluminium carbide layer at the carbon-metal interface. The thicker layer of B may be explained by its permeability that is roughly 60% higher than the one of grade C, thus allowing more bath species to infiltrate and

further react according to reaction 2. In this way, the thickness of the aluminum carbide layer may be affected by the combination of both open porosity and air permeability of the cathode block. This is shown with the case of grades B and E that have similar porosity, permeability and carbide thickness. The high amount of sludge in grade A may explain the thinner than expected carbide layer. This could be attributed to a combination of two phenomena. The high presence of sludge reduces carbides formed by Eq. 1. Moreover, sludge areas corresponding to lower current density lessens sodium intercalation and carbides formed by Eq. 2. The second phenomenon being aluminum carbide dissolution in sludge.
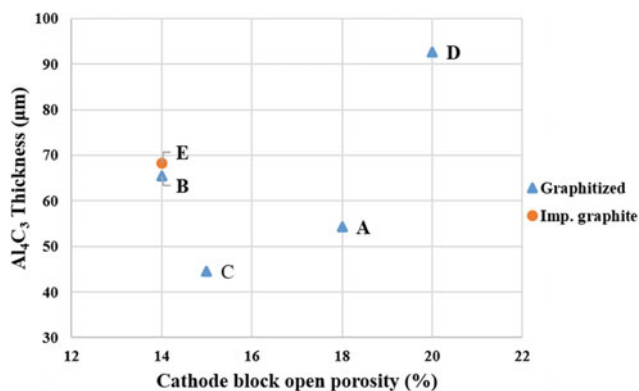
Central Sludge

The presence of a central sludge deposit at the carbon-aluminium interface was not foreseeable since there was no direct feeding of alumina during all experiments. The absence of point feeding or anode change in this study insinuates that sludge may come from other phenomena.

Considering that the cell dimensions are too short for considerable MHD forces, only the generated gas at the anode tip will agitate the layer of bath and the metal pad. The detachment of metal from the main pad may lead to the access of some bath to the carbon-aluminium interface. A proof of this agitation was obtained by running a test during which the electrolysis was maintained during cooling until the entire system was solid. The agitated metal may also

Fig. 4 Thickness of the aluminium carbide layer at the carbon-aluminium interface of the five experimental cells (triangles: graphitized blocks; circle: impregnated graphite)

cause the tip of the ledge toe to be dragged towards the center of the carbon-aluminium interface (under the anode), contributing to the accumulation of sludge. In this experimental study, the sludge may well come from ledge by agitation since Table 3 shows that the composition of the sludge and ledge are close. Furthermore, for a grade with thick ledge such as A, there is a film of bath connecting the central sludge to the ledge toe visible on Fig. 3a. Its CR and alumina content are respectively 2.49 and 24.3%, very similar to the ledge toe but higher than the sludge (see Table 3). The lower alumina content and CR of the central sludge in cell A may be explained by back feeding of alumina into the film and acidification through sodium loses [13].

Knowing that the side ledge and ledge toe are formed when their temperatures reaches a value below the liquidus of the bath, in that regard the thermal conductivity of the block may affect the extent of ledge toe elongation, thus the amount of sludge.

Conclusions

Aluminium Carbide Behaviour

The higher porosity of graphite deepens the reacting zone of infiltrated bath components, thus enlarging the apparent thickness of the carbide layer. Furthermore, the permeability of the carbon block may enhance the effect of porosity. On the contrary, the presence of sludge at the carbon-aluminium interface reduces the thickness of the aluminium carbide layer by diminution of current density and dissolution of the carbides in the sludge. For graphitized grades, a thinner carbide layer can be obtained with blocks that have a low porosity, a low permeability and a high tendency to form sludge.

Sludge Formation

This study has shown that sludge may form even without alumina point feeding or any manipulation with the anode.

The behavior of the five grades was not the same in experimental tests than in industrial cells regarding sludge propensity. The comparison between the laboratory tests with the industrial cell behavior of these grades regarding sludge formation is still under investigation. It may be achieved by further investigating the impact of other operating conditions such as feeding strategy or electrolysis time.

Analyses of sludge deposits suggest that the thermal conductivity of the carbon block may influence the amount of ledge, which can be transported along the carbon-aluminium interface by metal agitation.

References

1. Geay, P.-Y., B.J. Welch, and P. Homsi: Sludge in operating aluminum smelting cells, *Light Metals 2001*, 541–548.
2. Keller R.: Alumina dissolution and sludge formation revisited, *Light Metals 2005*, 147–150.
3. Wang, Z., et al. Cathode Wear in Electrowinning of Aluminum Investigated by a Laboratory Test Cell, *Light Metals 2016,* 897–902.
4. Novak, B., et al.: Fundamentals of aluminium carbide formation, *Light Metals 2012*, 1343–1348.
5. Coulombe, M.-A., et al. (2016), Factors Leading to the Formation of a Resistive Thin Film at the Bottom of Aluminum Electrolysis Cells, *Metall. Mater. Trans. B*, 1280–1295, https://doi.org/10.1007/s11663-015-0567-8.
6. Tschöpe, K., et al.: Critical reflections on laboratory wear tests for ranking commercial cathode materials in aluminium cells, *Light Metals 2013*, 1251–1256.
7. Zoukel, A., P. Chartrand, and G. Soucy: Study of Aluminum Carbide Formation in Hall-Heroult Electrolytic Cells, *Light Metals 2009*, 1123–1128.
8. Dassylva-Raymond, V., et al.: Modeling the Behavior of Alumina Agglomerate in the Hall-Heroult Process, *Light Metals 2014*, 603–608.
9. James, B.J., et al. (1995): Interfacial Processes and the Performance of Cathode Linings in Aluminum Smelters, *JOM,* 22–25, https://doi.org/10.1007/BF03221401.
10. Allard, F., G. Soucy, and L. Rivoaland (2014): Formation of Deposits on the Cathode Surface of Aluminium Electrolysis Cells, *Metall. Mater. Trans. B*, 2475–2485, https://doi.org/10.1007/s11663-014-0118-8.
11. Siew, E.F., et al.: A study of the fundamentals of pothole formation, *Light Metals 2005*, 763–769.
12. Einarsrud, K.E., E. Skybakmoen, and A. Solheim: On the influence of MHD driven convection on cathode wear, *Light Metals 2014*, 485–490.
13. Whitfield, D., et al.: Aspects of alumina control in aluminium reduction cells, *Light Metals 2004*, 249–255.